

Genetic analysis of CAND1–CUL1 interactions in *Arabidopsis* supports a role for CAND1-mediated cycling of the SCF^{TIR1} complex

Wenjing Zhang*, Hironori Ito*, Marcel Quint*, He Huang*, Laurent D. Noël^{†‡}, and William M. Gray^{*§}

*Department of Plant Biology, University of Minnesota–Twin Cities, St. Paul, MN 55108; and [†]Institut de Biologie Environnementale et Biotechnologie, Unité Mixte de Recherche 6191 Centre National de la Recherche Scientifique–Commissariat à l'Énergie Atomique–Université de la Méditerranée Aix-Marseille II, F-13108 Saint Paul-lez-Durance Cedex, France

Communicated by Mark Estelle, Indiana University, Bloomington, IN, April 29, 2008 (received for review February 18, 2008)

SKP1-Cullin1-F-box protein (SCF) ubiquitin-ligases regulate numerous aspects of eukaryotic growth and development. Cullin-Associated and Neddylation-Dissociated (CAND1) modulates SCF function through its interactions with the CUL1 subunit. Although biochemical studies with human CAND1 suggested that CAND1 plays a negative regulatory role by sequestering CUL1 and preventing SCF complex assembly, genetic studies in *Arabidopsis* have shown that *cand1* mutants exhibit reduced SCF activity, demonstrating that CAND1 is required for optimal SCF function *in vivo*. Together, these genetic and biochemical studies have suggested a model of CAND1-mediated cycles of SCF complex assembly and disassembly. Here, using the SCF^{TIR1} complex of the *Arabidopsis* auxin response pathway, we test the SCF cycling model with *Arabidopsis* mutant derivatives of CAND1 and CUL1 that have opposing effects on the CAND1–CUL1 interaction. We find that the disruption of the CAND1–CUL1 interaction results in an increased abundance of assembled SCF^{TIR1} complex. In contrast, stabilization of the CAND1–CUL1 interaction diminishes SCF^{TIR1} complex abundance. The fact that both decreased and increased CAND1–CUL1 interactions result in reduced SCF^{TIR1} activity *in vivo* strongly supports the hypothesis that CAND1-mediated cycling is required for optimal SCF function.

auxin | SCFTIR1 | ubiquitin-ligase | COP9 signalosome

The ubiquitin/26S proteasome pathway regulates numerous aspects of plant growth and development. SKP1-Cullin1-F-box protein (SCF) complexes comprise the largest class of ubiquitin-ligases in *Arabidopsis* (1). These multisubunit enzymes consist of four subunits: the RING protein RBX1 binds to a C-terminal domain of the CUL1 scaffold protein, whereas the SKP1 adaptor protein binds to the N terminus of CUL1. The fourth subunit is any of several F-box proteins (FBPs) that bind SKP1 via their F-box domain. FBPs act as recognition factors to recruit specific substrates to the SCF complex for ubiquitination. With ≈ 700 FBP genes in the *Arabidopsis* genome, plants have the capacity to assemble many distinct SCF complexes, which likely play a prominent role in regulating many biological processes (1).

SCF^{TIR1} contains the TIR1 FBP and regulates response to the plant hormone auxin by targeting repressors of auxin response known as Aux/IAA proteins for ubiquitin-mediated proteolysis (2). Several additional plant FBPs have been implicated in a diverse range of biological processes, including hormonal signaling, photomorphogenesis, organ development, self-incompatibility, defense response, and circadian clock control (3). How plants and other eukaryotes regulate this multitude of FBPs assembling with a common CUL1-RBX1 core complex to form distinct SCF complexes for controlling the stability of hundreds of substrates is unclear.

Studies in numerous eukaryotes have shown that the conjugation of the ubiquitin-like protein RUB/NEDD8 to the CUL1 subunit is required for optimal SCF ubiquitin-ligase activity (4–6). In *Arabidopsis*, mutations affecting the RUB-

modification pathway reduce SCF^{TIR1} activity, resulting in the stabilization of Aux/IAA proteins and diminished auxin response (7, 8). *In vitro* assays demonstrate that modification increases SCF activity (6, 9) possibly by facilitating the recruitment of E2-ubiquitin conjugates to the SCF complex (10). Hypermodification of CUL1 also disrupts SCF^{TIR1} function *in vivo* (11), and cleavage of RUB off CUL1 by the COP9 signalosome (CSN) is required for optimal SCF activity. Although purified CSN inhibits SCF activity *in vitro* by removing RUB from CUL1, SCF substrates accumulate in CSN-deficient mutants, indicating reduced SCF activity *in vivo* (12). Together these findings suggest that RUB modification of CUL1 is highly dynamic, with cycles of RUB conjugation and removal being required for proper SCF activity.

Discovery of the human Cullin-Associated and Neddylation-Dissociated (CAND1) protein suggested how cycles of RUB conjugation and cleavage might regulate SCF activity. Biochemical studies found that CAND1 specifically binds unmodified CUL1 to form a ternary complex with the CUL1-RBX1 SCF catalytic core (13, 14). Because CAND1 binding precludes CUL1 from binding SKP1, CAND1 was proposed to act as a negative regulator of SCF complex assembly by sequestering CUL1. Because CAND1 only binds unmodified CUL1, a model invoking cycles of RUB modification and cleavage was proposed to modulate interactions between CUL1 and CAND1 to regulate SCF complex assembly (12). However, more recent biochemical and structural studies suggest that RUB conjugation occurs after SCF complex assembly (15, 16), raising new questions about the regulation of CAND1–CUL1 interactions.

Although these *in vitro* studies suggested that CAND1 acts as a negative regulator of SCF complexes, the identification of *cand1* mutants in *Arabidopsis* indicated otherwise. Loss-of-function mutations in CAND1 confer multiple defects in growth and development, including reductions in auxin response and other SCF-regulated processes (17, 18). Furthermore, IAA7, an SCF^{TIR1} substrate, and RGA, an SCF^{SLY1} substrate, exhibit increased stability in *cand1* mutants, clearly indicating that CAND1 positively regulates SCF function *in vivo*. These genetic findings can be reconciled with the *in vitro* data, however, if cycles of SCF assembly and disassembly are required for proper SCF activity *in vivo* (12). Such a requirement would explain how mutations in factors hypothesized to promote SCF disassembly,

Author contributions: W.Z., H.I., M.Q., H.H., and W.M.G. designed research; W.Z., H.I., M.Q., H.H., and W.M.G. performed research; L.D.N. contributed new reagents/analytic tools; W.Z., H.I., M.Q., H.H., and W.M.G. analyzed data; and W.Z. and W.M.G. wrote the paper.

The authors declare no conflict of interest.

[†]Present address: Laboratoire des interactions plantes micro-organismes, F-31326 Castanet-Tolosan, France.

[§]To whom correspondence should be addressed. E-mail: grayx051@tc.umn.edu.

This article contains supporting information online at www.pnas.org/cgi/content/full/0804144105/DCSupplemental.

© 2008 by The National Academy of Sciences of the USA

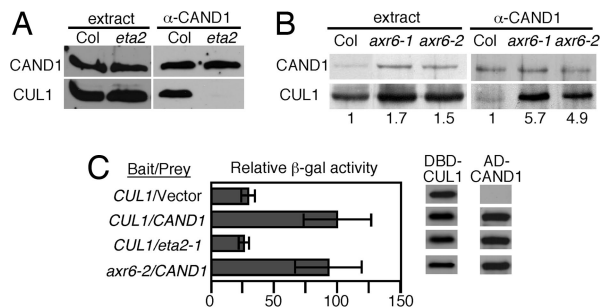


Fig. 1. Effects of the *eta2-1* and *axr6-2* mutations on CAND1–CUL1 interactions. (A and B) α -CAND1 antibody was used to precipitate CAND1 from Col, *eta2-1*, *axr6-1*, and *axr6-2* seedling extracts. Precipitates were immunoblotted with CAND1 and CUL1 antisera. Densitometric quantification of CUL1 levels in the extracts and precipitates relative to Col are shown below each lane in B. (C) (Left) CAND1–CUL1 yeast 2-hybrid assays. β -gal activities are expressed relative to wild type. Error bars indicate SD ($n = 3$). (Right) Western blots of yeast extracts expressing the bait and prey constructs.

such as CAND1 and the CSN, could result in reduced SCF activity. Because many FBPs compete for access to a common CUL1–RBX1 catalytic core, SCF cycling may provide plasticity to a cell's complement of assembled SCF complexes. Cycling also has been proposed to protect FBP subunits from autoubiquitination in the absence of available substrates and could conceivably provide a mechanistic basis for promoting the preferential incorporation of FBP–substrate complexes into the SCF or the release of ubiquitinated substrates.

As a genetic test of the SCF cycling hypothesis, we characterized SCF^{TIR1} assembly and function in *Arabidopsis cand1* and *cull1* mutants that differentially affect the CAND1–CUL1 interaction. Our results support the cycling model and demonstrate that CAND1–CUL1 interaction dynamics play a crucial role in the control of SCF activity *in vivo*.

Results

Opposing Effects of *eta2-1* and *axr6-2* on CAND1–CUL1 Interactions. We have previously described a *CAND1* mutant, *eta2-1*, that contains a missense mutation within a highly conserved region near the C terminus (17). *eta2-1* plants exhibit diminished SCF^{TIR1} activity and a corresponding reduction in auxin response. To examine how the mutation affects CAND1 function, we examined interactions between CAND1 and CUL1 by using coimmunoprecipitation assays. As previously reported, the *eta2-1* mutation had no effect on CAND1 or CUL1 protein levels (Fig. 1A). However, although unmodified CUL1 efficiently coprecipitated with CAND1 from wild-type extracts, little if any CUL1 was observed in α -CAND1 precipitates from *eta2-1* extracts (Fig. 1A). Thus, the *eta2-1* point mutation greatly diminishes the ability of CAND1 to bind CUL1. Consistent with this finding, the *eta2-1* mutation completely abolished the ability of CAND1 to interact with CUL1 in a yeast 2-hybrid assay (Fig. 1C).

axr6-1 and *axr6-2* are dominant-negative alleles of *CUL1* that confer reduced auxin response when heterozygous and a seedling-lethal phenotype when homozygous (19). These two mutations are distinct missense alleles of the same amino acid in an N-terminal domain of CUL1 that is involved in both SKP1 and CAND1 binding (16). To investigate how *axr6-1* and *axr6-2* affect the CAND1–CUL1 interaction, we performed α -CAND1 immunoprecipitations with wild-type and homozygous mutant seedling extracts. In both *axr6* mutants, we detected a dramatic increase in the amount of CUL1 coprecipitating with CAND1 (Fig. 1B). Like wild-type CUL1, however, the interaction was abolished by the *eta2-1* mutation [supporting information (SI)

Fig. S1A]. To investigate the possibility that *axr6-2* increases affinity for CAND1, we examined the interaction in a yeast 2-hybrid system. In contrast to our results with plant extracts, *axr6-2* did not obviously affect interactions with CAND1 in yeast (Fig. 1C). A possible explanation for this difference is that *Saccharomyces cerevisiae* does not contain a CAND1 ortholog. Thus, there may be factors regulating CAND1–CUL1 interactions in higher eukaryotes that are absent from the yeast 2-hybrid system.

***eta2-1* and *axr6-2* Differentially Affect SCF^{TIR1} Complex Abundance.** If CAND1 regulates cycles of SCF assembly and disassembly by binding to CUL1, this cycle should be disrupted in *eta2-1* and *axr6-2* mutants. To test this possibility, we examined the SCF^{TIR1} complex in *eta2-1* mutants by using a gel-filtration assay. A construct containing the *TIR1* promoter driving expression of a *TIR1*–HA–Strep-tagged transgene was introduced into *tir1-1* plants. This transgene fully complemented the auxin response defects conferred by the *tir1-1* mutation (L.D.N., unpublished data). The transgene was subsequently crossed into the *tir1-1 eta2-1* background, and α -HA Western blots confirmed equivalent levels of TIR1–HA–Strep expression (Fig. 2A). Protein extracts of *tir1-1*[*TIR1*–HA–Strep] and *tir1-1 eta2-1*[*TIR1*–HA–Strep] (subsequently referred to as “wild-type control” and “*eta2-1*,” respectively) were fractionated and blotted with antibodies against CAND1, CUL1, HA, and ASK1 (*Arabidopsis SKP1*).

In wild-type extracts, the \approx 135-kDa CAND1 protein was detected predominantly in fractions 10–14, corresponding to molecular masses of \approx 100–350 kDa (Fig. 2B). The CAND1–CUL1–RBX1 (CCR) complex has a predicted molecular mass of \approx 235 kDa. The major CUL1 peak cofractionated with the upper distribution of CAND1 (Fig. 2B). Consistent with our findings that the *eta2-1* mutation prevents CUL1 binding, the mutant protein was only detected in the low-molecular mass fractions (Fig. 2B). Thus, the CCR complex is present predominantly in fractions 10 and 11.

Surprisingly, the CUL1 elution profile was unaltered by the *eta2-1* mutation (Fig. 2B). However, SCF complexes have a predicted molecular mass very similar to that of the CCR complex. Because CUL1 assembles into the CCR and SCF complexes in a mutually exclusive fashion, it seemed possible that the disruption of the CCR complex by the *eta2-1* mutation results in more CUL1 assembling into SCF complexes, which would be consistent with the predictions of the SCF cycling model. Consistently, we found that the *eta2-1* mutation results in an enrichment of TIR1 in fractions corresponding to the molecular mass of the SCF^{TIR1} complex. The majority of TIR1 from wild-type extracts eluted in low-molecular-mass fractions the size of monomeric TIR1 or a TIR1–ASK complex (Fig. 2B). In contrast, TIR1 was nearly equally distributed between these low-molecular-mass fractions and fractions 10–11 in *eta2-1* extracts. The *eta2-1* mutation also caused a consistent increase in the relative amount of ASK1 that coeluted with CUL1 and TIR1 in fractions 10 and 11 (Fig. 2B). Together these results indicate that loss of the CCR complex in the *eta2-1* mutant results in an increased abundance of the SCF^{TIR1} complex.

Compared to *eta2-1*, the *axr6-2* mutation had opposing effects on CCR and SCF complex abundance. A clear shift in the CAND1 elution profile was consistently observed, with more CAND1 coeluting with CUL1 in fractions 10 and 11 containing the CCR complex (Fig. 2B). Additionally, consistent with previous coimmunoprecipitation experiments indicating that the *axr6-2* mutation dramatically reduced interactions with ASK1 (19), we find *axr6-2* causes a reduction in the relative abundance of ASK1 that coelutes with CUL1 in SCF fractions 10 and 11 (Fig. 2B). In a yeast 2-hybrid assay, however, *axr6-2* caused only a moderate reduction in the ability to interact with ASK1 (Fig.

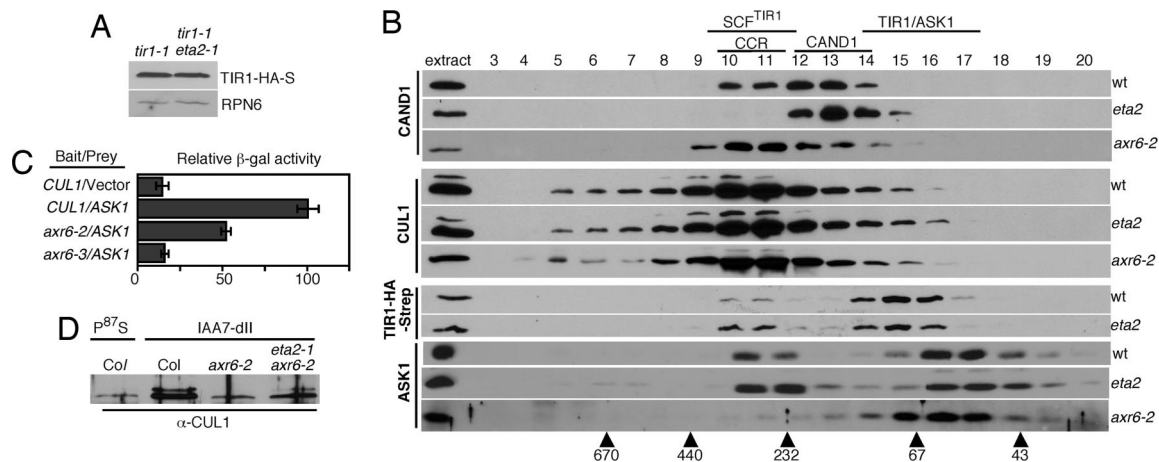


Fig. 2. Effects of the *eta2-1* and *axr6-2* mutations on CCR and SCF complex abundance. (A) α -HA Western blot of *tir1-1*[P_{TIR1} ::TIR1-HA-Strep] and *tir1-1 eta2-1*[P_{TIR1} ::TIR1-HA-Strep] seedling extracts. RPN6 is shown as a loading control. (B) Extracts from 7-day-old seedlings were fractionated on a Superdex-200 gel-filtration column and fractions (1–20) were collected and blotted with α -CAND1, α -CUL1, α -HA, and α -ASK1 antibodies. Molecular mass standards are labeled at the bottom. (C) CUL1-ASK1 2-hybrid assays. β -gal activities are expressed relative to wild type. Error bars indicate SD ($n = 3$). *axr6-3* is shown as an additional negative control. (D) A 6 \times His fusion protein containing IAA7 domain II (amino acids 71–100) was incubated with and subsequently purified from 1.5 mg of 7-day-old seedling extracts. A derivative containing the P⁸⁷S mutation, which abolishes TIR1 binding, was used as a negative control. Pulldowns were immunoblotted with antisera against CUL1.

2C). Together these findings suggest that the *axr6-2* mutation may shift the CUL1-binding equilibrium in favor of CAND1, thus reducing SCF complex assembly. To further test this possibility, we performed pull-down assays with plant extracts by using a domain II peptide from IAA7, an SCF^{TIR1} substrate (8). Consistent with there being less assembled SCF^{TIR1}, the *axr6-2* mutation resulted in a reduction in the amount of CUL1 protein pulled down by the domain II bait peptide. However, CUL1 binding was partially restored in *eta2-1 axr6-2* double mutants (Fig. 2D).

Loss of CAND1 Suppresses *axr6-2*. To test the possibility that the *axr6-2* mutation prevents CAND1–CUL1 dissociation, we generated double mutants with *eta2-1*. *eta2-1* suppressed the seedling-lethal phenotype of *axr6-2* homozygotes (Fig. 3A). Additionally, although *eta2-1* is recessive, its suppression of *axr6-2* is dominant, indicating increased sensitivity to CAND1 dosage. Examination of auxin inhibition of root growth revealed that *eta2-1 axr6-2* double mutants display only a weak auxin response defect comparable to *eta2-1* single mutants (Fig. S1B). Like *eta2-1*, the *cand1-1*-null allele (18) also suppressed the lethality of *axr6-2* in a dominant fashion (Fig. 3B), indicating that suppression is not allele-specific, but is simply due to loss of CAND1 function. Thus, in the absence of CAND1, the *axr6-2* mutant protein must be capable of fulfilling most, if not all, CUL1 functions. Curiously, although *cand1-1* was largely epistatic to *axr6-2*, the *axr6-2* mutation partially suppressed the dwarf phenotype of *eta2-1* (Fig. 3A and B).

In addition to suppressing the lethality of *axr6-2*, mutations in *cand1* also suppress the effects of *axr6-2* on the cullin protein. As previously reported (19), *axr6-1* and *axr6-2* cause a modest increase in the CUL1 protein level and a decrease in the ratio of RUB modified to unmodified CUL1, implying a defect in RUB modification. However, the loss of CAND1 restores both wild-type cullin levels and normal RUB modification to *axr6-1* and *axr6-2* plants (Fig. 3C).

Loss of CAND1 Enhances *axr6-3*. Unlike the dominant CUL1 alleles described above, *axr6-3* is a recessive, temperature-sensitive mutation. We have previously shown that this mutation prevents SCF assembly by abolishing ASK1 binding, but does not affect interactions with CAND1 (20). In sharp contrast to the suppres-

sion seen with *axr6-2*, *eta2-1 axr6-3* double mutants displayed very dramatic phenotypes. All double mutant plants died when grown at 28°C (Fig. 4A and B). When grown at the more permissive temperature of 18°C, a few double mutants survived to adulthood, but exhibited extreme dwarfism, delayed senescence, and complete sterility (Fig. 4C and D). Auxin response assays of *eta2-1 axr6-3* double mutants revealed that, although *eta2-1* enhances the auxin response defect of *axr6-3* at semipermissive temperature (data not shown), *axr6-3* is largely epistatic to *eta2-1* at higher temperatures (Fig. 4E). This finding is consistent with our previous finding that *axr6-3* prevents SCF assembly at 28°C (20). Thus, the severe growth defects of *eta2-1 axr6-3* double mutants may be due to the effects of *eta2-1* on

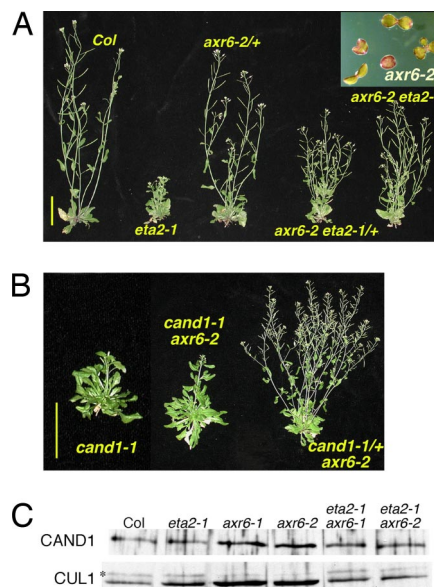


Fig. 3. Genetic interaction between *eta2* and *axr6-2*. (A and B) Adult phenotypes of single and double mutants. (Inset) Terminal seedling-lethal phenotype of CAND1⁺ *axr6-2* homozygotes. (Scale bars: 5 cm.) (C) α -CAND1 and α -CUL1 protein Western blots of 6-day-old seedling extracts. CUL1-RUB is indicated with an asterisk.

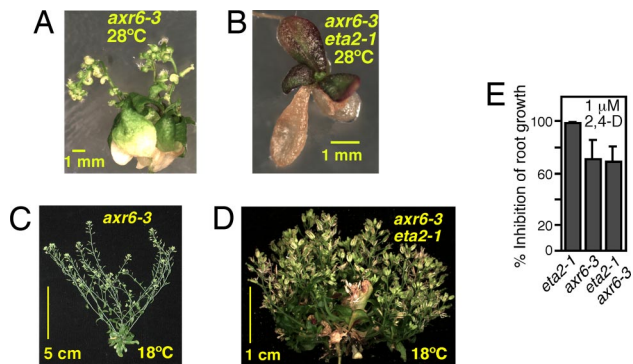


Fig. 4. Genetic interactions between *eta2-1* and *axr6-3*. (A and B) Forty-two-day-old *axr6-3* and *axr6-3 eta2-1* plants grown at 28°C. The double mutant fails to develop further after forming two to three pairs of true leaves. (C and D) Adult phenotypes of *axr6-3* and *axr6-3 eta2-1* double mutants grown at 18°C. (E) Inhibition of root elongation by 2,4-D. Seedlings grown at 20°C were transferred to 1 μ M 2,4-D medium and grown an additional 4 days at 28°C. Error bars indicate SD ($n \geq 12$).

CUL3- and CUL4-based ubiquitin ligases (21, 22), rather than further impairment of CUL1-based SCF complexes.

***eta2-1* Enhances a Weak Mutation in the CSN.** The *eta6* mutant was isolated from the same *tir1-1* enhancer screen used to isolate *eta2-1* (17). Map-based cloning revealed that *eta6* is a recessive allele of *CSN1/FUS6*, which encodes a subunit of the CSN (23). This finding was confirmed by allelism tests with *fus6-1* and by complementation with a *CSN1* transgene, prompting us to rename our mutant *csn1-10* (Fig. 5A). *csn1-10* is a transition

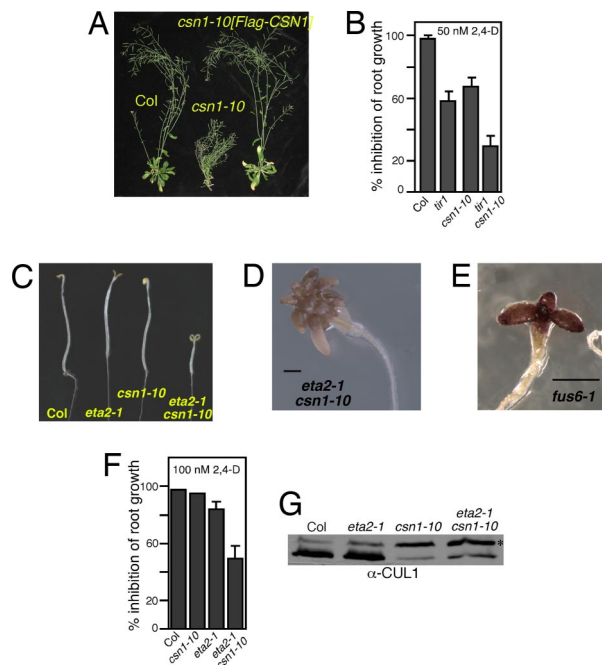


Fig. 5. Genetic interactions between *eta2-1* and *csn1-10*. (A) Adult Col, *csn1-10*, and *csn1-10[FLAG-CSN1]* plants. (B) Auxin-resistant root growth of *csn1-10* and *csn1-10 tir1-1* seedlings. Seedlings were transferred to 50 nM 2,4-D and grown an additional 4 days. Error bars indicate SD ($n \geq 10$). (C) Seven-day-old etiolated seedlings. (D) Sixty-day-old *eta2-1 csn1-10* double mutants. (E) Twenty-one-day-old *fus6-1* seedling. Seedlings do not develop further. (F) Root growth assay on medium containing the synthetic auxin 2,4-D. Error bars indicate SD ($n \geq 12$). (G) α -CUL1 Western blot of 11-day-old seedling extracts. CUL1-RUB is indicated with an asterisk. (Scale bars: 1 mm.)

mutation resulting in a Ser \rightarrow Asn substitution at amino acid 305 (Fig. S2A). This residue is highly conserved among eukaryotic CSN1 orthologs. However, this mutation is in the last base of exon 4 and also affects mRNA splicing. Our analysis of *CSN1* transcripts from *csn1-10* plants detected two mRNA species: one that was correctly spliced and a second produced by using an errant splice site 32 bases upstream, resulting in a short deletion followed by a frameshift that truncates the protein. Western analysis revealed a reduction in the level of full-length CSN1 protein, but we did not detect the truncated derivative (Fig. S2B). At this time, we do not know whether the *csn1-10* phenotypes are the result of the missense mutation, the reduction in CSN1 levels due to the splicing error, or a combination of both.

Previous screens for constitutive photomorphogenesis/de-etiolated/*fusca* (*cop/det/fus*) mutants have identified *CSN1* and several other CSN subunit mutations (24). All of these mutants exhibit a strong *cop⁻* phenotype when grown in the dark and are seedling-lethal. Unlike these previously characterized *csn* mutants, *csn1-10* does not display a *cop⁻* phenotype and is viable throughout development (Fig. 5A and C). *csn1-10* seedlings do, however, exhibit auxin-resistant root growth (Fig. 5B) and reduced SCF^{TIR1} activity (Fig. S2C). These findings suggest that *csn1-10* is a weak allele that must retain sufficient CSN function for viability and repression of photomorphogenesis.

Because the CSN has been proposed to act in conjunction with CAND1 to regulate cullins, we generated *csn1-10 eta2-1* double mutants to examine genetic interactions. While *cand1* single mutants exhibit only a weak *cop⁻* phenotype (17, 18), *eta2-1 csn1-10* double mutants display a much stronger de-etiolation defect (Fig. 5C). When grown in the light, double mutants produced several pairs of very small leaves, but never transitioned into reproductive development (Fig. 5D). This phenotype is similar to severe *csn* mutants, although *csn*-null plants generally produce only a few pairs of leaves before arresting (Fig. 5E). The *csn1-10* mutation causes a modest increase in the auxin response defect conferred by *eta2-1* (Fig. 5F).

The CSN regulates SCF function via its metalloisopeptidase activity that cleaves RUB from CUL1 (25). CUL1 Western blots revealed a clear accumulation of RUB-modified CUL1 in *csn1-10* seedling extracts. However, this defect was not enhanced by *eta2-1* (Fig. 5G). Likewise, gel-filtration analysis of CSN4 and CSN5 (Fig. S2D) revealed that the *eta2-1* mutation does not affect the elution profile of these subunits, suggesting that CSN assembly and interactions are not dependent on CAND1.

Discussion

Arabidopsis cand1 mutants exhibit several auxin response defects resulting from a reduction in SCF^{TIR1} activity (17, 18). Although genetic studies indicate that CAND1 positively regulates SCF^{TIR1} function, biochemical studies on human CAND1 suggested that it negatively regulated SCF assembly by sequestration of the CUL1 subunit. *In vivo*, SCF complexes are likely to be highly dynamic because many FBPs compete for access to a common CUL1-RBX1 catalytic core. Thus, if CAND1 facilitates cycles of SCF assembly and disassembly, the loss of CAND1 could result in reduced SCF activity. The SCF cycling model proposed that active SCF complexes containing RUB/NEDD8-modified CUL1 recruit the CSN, which removes RUB from CUL1 (12). Because CAND1 specifically binds unmodified CUL1, RUB cleavage could enable CAND1 to bind the CUL1-RBX1 core and dissociate the SCF. Although remodeling of CUL1 was initially proposed to free CUL1 from CAND1 and promote SCF reassembly, recent findings, including this study, indicate that RUB modification occurs after CUL1 has been released from CAND1 and has assembled an SCF complex (15, 16). Using the genetic tools provided by *Arabidopsis CUL1*,

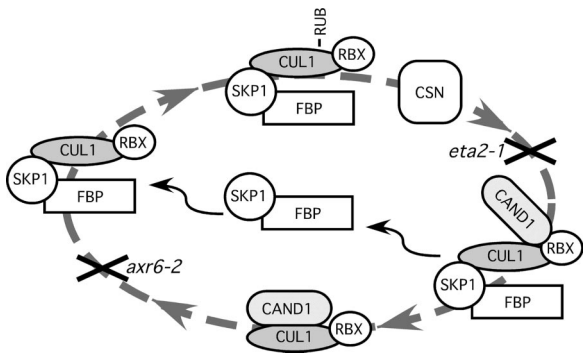


Fig. 6. CAND1-mediated cycling. An active SCF complex containing RUB-modified CUL1 is shown at the top. After CSN-mediated RUB cleavage, CAND1 promotes SCF disassembly by dissociating CUL1-RBX1 from SKP1-FBP. SCF disassembly is blocked in the *eta2-1* mutant, resulting in SCF complex accumulation. Dissociation of CUL1-RBX1 from CAND1 reassembles the SCF. However, this process is blocked in *axr6-2* mutants. Upon release from CAND1 and SCF reassembly, the CUL1 subunit is RUB-modified, activating the SCF for substrate ubiquitination.

CAND1, and *CSN* mutants, we have tested several aspects of this model.

The *eta2-1* and *axr6-2* mutations differentially affect CAND1–CUL1 interactions and SCF^{TIR1} homeostasis. *eta2-1* (17) and *axr6-2* (19) are both single amino acid missense mutations located in close proximity within the CUL1–CAND1 interface (16). We demonstrate that these two mutations have opposing effects on CAND1–CUL1 interactions. Whereas the CAND1–CUL1 interaction is largely abolished by the *eta2-1* mutation, a dramatic increase in CAND1–CUL1 complex abundance is seen in *axr6-2* mutants.

Biochemical studies with human CAND1 found that its binding to CUL1 is antagonistic to SKP1 binding, suggesting that CAND1 negatively regulates SCFs by sequestering CUL1 to prevent SCF complex assembly (13, 14). Our studies of *eta2-1* and *axr6-2* mutants support this negative role for CAND1 in regulating SCF assembly. Our gel-filtration assays reveal that the reduced CAND1–CUL1 interaction in *eta2-1* mutants results in the accumulation of the SCF^{TIR1} complex (Fig. 2B). This conclusion is further supported by our previous results of IAA7 pull-down assays, which detected an increase in the relative amount of CUL1 pulled down from *eta2-1* extracts compared with wild-type controls (17). In contrast, *axr6-2* has a stabilizing effect on the CAND1–CUL1 complex, leading to a reduction in SCF assembly, as we observed diminished abundance of ASK1 in gel-filtration fractions corresponding to SCF complexes in *axr6-2* extracts. Furthermore, noticeably less CUL1 copurified with an IAA7 bait protein in pull-down assays with *axr6-2* extracts (Fig. 2D). This reduction was dependent on CAND1 because the *eta2-1* mutation partially restored the amount of CUL1 copurifying with IAA7. Despite these opposing effects on SCF^{TIR1} assembly, both *eta2-1* and *axr6-2* confer reduced SCF^{TIR1} activity as indicated by the stabilization of Aux/IAA protein substrates and reduced sensitivity to auxin (17, 19), strongly supporting the hypothesis that CAND1-mediated cycling is required for optimal SCF^{TIR1} activity *in vivo* (Fig. 6).

The effects of the dominant-negative *axr6-1* and *axr6-2* mutations on CUL1 are very interesting. These two missense mutations change Phe¹¹¹ to Trp and Ile residues, respectively. Previous CUL1 coimmunoprecipitation experiments with plant extracts suggested that these mutations reduce interactions with the ASK1 SCF subunit (19). Such a defect does not explain the dominant nature of these mutations however, because *axr6-3* also is defective in ASK1 binding, but is recessive (20). Our findings that *axr6-1* and *axr6-2* cause a striking increase in the

relative amount of CUL1 associated with CAND1 provides an explanation because the stabilized *axr6-2*–CAND1 complex could disrupt SCF cycling in *AXR6/axr6-2* heterozygotes, preventing wild-type CUL1 from reassembling into SCF complexes efficiently. Thus, the previously reported strong reduction in ASK1 binding activity may largely be due to the inability of the mutant *axr6-2* protein to dissociate from CAND1. Our double-mutant studies strongly support this possibility. Whereas *axr6-2* homozygous plants exhibit a seedling-lethal phenotype, double mutants with *cand1* are viable and only exhibit a weak auxin response defect comparable to *cand1* single mutants. This clearly demonstrates that the lethality conferred by *axr6-2* is dependent on *CAND1* and that, in the absence of *CAND1*, *axr6-2* has minimal effects on SCF activity.

The suppression of the RUB modification defect of *axr6-1* and *axr6-2* also suggests that these *cull1* mutations block CAND1–CUL1 dissociation. The finding that *axr6-1* and *axr6-2* mutations confer reduced RUB modification despite these lesions being near the N terminus of the protein while RUB modification occurs near the C terminus (4) has previously been difficult to explain. Although loss of CAND1 does not alter the RUB modification profile of wild-type CUL1 (17, 18), *cand1* mutations restore RUB modification to *axr6-1* and *axr6-2*. This finding provides genetic support that CAND1 inhibits RUB modification of CUL1, as suggested by recent structural and biochemical studies of the human CCR complex (15, 16). This work highlights the question of what regulates CAND1–CUL1 dissociation. *In vitro* studies indicate that the addition of SKP1-FBP to preassembled CAND1–CUL1 complexes can promote dissociation (15). However, there also is evidence that an additional, unknown CUL1-associated factor may play an important role because the effect of SKP1-FBP addition is noticeably stronger with fractionated CUL1 versus recombinant CUL1 (15, 16). Our findings that *axr6-2* “traps” CUL1 in the CAND1 complex without dramatically affecting CUL1 interactions with either CAND1 or ASK1 in yeast 2-hybrid assays are consistent with this possibility. The finding that *axr6-3* completely abolishes ASK1 binding, but does not increase CAND1–CUL1 abundance (20), also suggests that *axr6-2* may specifically inhibit dissociation.

Genetic Interactions with the CSN. CAND1 is thought to act in concert with the CSN to regulate SCF disassembly (12). Previously described *csn* subunit mutants exhibit strong de-etiolation and seedling-lethal phenotypes. We isolated a weak *csn1* allele that is viable and remains etiolated when grown in the dark, thus providing a genetic tool for future studies investigating CSN-mediated regulation of signaling processes beyond the seedling stage. The *csn1-10* mutation moderately enhances the weak de-etiolation and auxin-resistant phenotypes of *cand1* mutants. However, overall growth and development are dramatically affected as *csn1-10 cand1* mutants exhibit extreme dwarfism and fail to transition into the reproductive phase of development. The fact that *csn*-null mutants are lethal and *csn1-10* enhances *cand1* suggests that these mutants are not simply impaired in CAND1-mediated cycling of cullin-based ubiquitin-ligases. Although both CAND1 and the CSN are thought to promote the disassembly of cullin-based ligases, only *csn* mutants are impaired in the RUB deconjugation from cullins. Previous studies in other systems have demonstrated that this defect of *csn* mutants can result in the autoubiquitination of FBPs, resulting in reduced SCF activity (26). Reduced FBP abundance also has been reported in animal cells in which *CAND1* expression has been knocked down using siRNA (14). However, we do not detect a reduction in TIR1 abundance (Fig. 2A) or stability (data not shown) in our *cand1* mutants. A separate study found that the endogenous levels of the *Arabidopsis* COI1 FBP were not affected by the loss of CAND1, but levels of an overexpressed UFO transgenic protein were diminished (18). Thus, although

the loss of *cand1* may not dramatically alter FBP stability, these mutants may be hypersensitive to perturbed CSN function. CAND1 may minimize the autoubiquitination of FBPs in *csn1-10* plants by facilitating SCF disassembly. In *csn1-10 cand1* double mutants, however, this protection may be lost, resulting in increased FBP autoubiquitination and severe defects in growth and development. Future studies need to address this possibility.

Materials and Methods

Plant Materials and Growth Conditions. All *Arabidopsis* lines used are in the Col-0 ecotype. Seedlings were grown under sterile conditions on ATS nutrient medium (27) under long-day lighting at 20°C. For coimmunoprecipitation experiments, seedlings were grown in liquid ATS medium on a shaker at 20°C. Adult plants were grown in soil under long-day conditions at 18°C or 20°C. For root growth assays, 4-day-old seedlings were transferred to ATS medium supplemented with 2,4-dichlorophenoxyacetic acid (2,4-D), and root growth was measured after an additional 4 days. The 35S::Flag-CSN1 transgene was provided by X. W. Deng (Yale University, New Haven, CT). To construct the *P_{TIR1}::TIR1-HA-Strep* transgene, a fragment containing 1.7 kb of upstream promoter sequence, the 5'-UTR, and the TIR1 coding sequence without the stop codon was amplified by PCR from Col-0 genomic DNA and cloned into the pExTag-HAStrep vector (28). The construct was subsequently transformed into *tir1-1* mutant plants by *Agrobacterium*-mediated transformation.

Yeast 2-Hybrid Assays. The full-length *CAND1* ORF was cloned into pJG4/5 (Origene) to make the prey construct. The pEG202-CUL1 bait construct was a gift from X. W. Deng (18). The K⁶⁸²R mutation in the RUB conjugation site and the *axr6-2* mutation were introduced into the CUL1 bait construct by using the QuikChange XL site-directed mutagenesis kit (Stratagene). These plasmids were cotransformed with the *P_{LexA}::lacZ* reporter pSH18-34 (31) into yeast strain EGY48. Transformed colonies were inoculated into liquid media lacking histidine, uracil, and tryptophan supplemented with 2% raffinose. Cells were

subcultured in 5 ml of the same media supplemented with 2% galactose to induce the expression of the *AD-CAND1* fusion. After 6–8 h growth, cells were harvested for liquid β -gal assays as described previously (29). For the CUL1-ASK1 assays, the constructs have been previously described (20). β -gal activities from the integrated *P_{GAL1}::lacZ* reporter in strain YPB2 were determined from cultures at 1.5×10^7 cells/ml grown at 24°C.

Antibodies, Immunoprecipitations, and Pull-Down Assays. CAND1, CUL1, and ASK1 antibodies have been described previously (17). HA monoclonal antibody was obtained from Covance Research Products. CSN4, CSN5, and RPN6 antibodies were purchased from Biomol. CAND1-CUL1 coimmunoprecipitations were performed as per Quint *et al.* (20) using extracts prepared from 5- to 7-day-old seedlings. The 6 \times His-IAA7-dll pull-down assays were performed as described previously (17).

Gel-Filtration Chromatography. Seven-day-old seedlings were homogenized in extraction buffer containing 50 mM Tris-HCl (pH 7.5), 150 mM NaCl, 10 mM MgCl₂, 1 mM EDTA, 10% glycerol, 1 mM DTT, 1 mM phenylmethylsulfonyl fluoride (PMSF), and 1 \times Halt protease inhibitors (Pierce). Homogenates were centrifuged for 15 min at 4°C to remove debris. Supernatants were spun again for 10 min and then filtered through a 0.2- μ m filter (Pall). Then 600 μ g of total protein was fractionated through a Superdex 200 10/300 GL column (Amersham). After loading the sample, proteins were eluted in filtered and degassed extraction buffer at a flow rate of 0.2 ml/min; 0.5-ml fractions were collected after the 6-ml void volume was reached and concentrated with StrataClean Resin (Stratagene). The column was calibrated by using gel-filtration calibration kits (Amersham) as per the manufacturer's instructions. All procedures were carried out at 4°C.

ACKNOWLEDGMENTS. We thank J. Cohen (University of Minnesota, St. Paul, MN) for providing an FPLC system. This work was supported by National Institutes of Health Grant GM067203 (to W.M.G.) and fellowships from the Deutsche Forschungsgemeinschaft (to M.Q.), Japanese Society for the Promotion of Science (to H.I.), and Bernard and Jean Phinney (to W.Z.).

- Smalle J, Vierstra RD (2004) The ubiquitin 26S proteasome proteolytic pathway. *Annu Rev Plant Physiol Plant Mol Biol* 55:555–590.
- Quint M, Gray WM (2006) Auxin signaling. *Curr Opin Plant Biol* 9:448–453.
- Lechner E, Achard P, Vansiri A, Potuschak T, Genschik P (2006) F-box proteins everywhere. *Curr Opin Plant Biol* 9:631–638.
- del Pozo JC, Estelle M (1999) The Arabidopsis cullin AtCUL1 is modified by the ubiquitin-related protein RUB1. *Proc Natl Acad Sci USA* 96:15342–15347.
- Lammer D, *et al.* (1998) Modification of yeast Cdc53p by the ubiquitin-related protein rub1p affects function of the SCFCdc4 complex. *Genes Dev* 12:914–926.
- Podust VN, *et al.* (2000) A Nedd8 conjugation pathway is essential for proteolytic targeting of p27Kip1 by ubiquitination. *Proc Natl Acad Sci USA* 97:4579–4584.
- del Pozo JC, *et al.* (2002) AXR1-ECR1-dependent conjugation of RUB1 to the Arabidopsis cullin AtCUL1 is required for auxin response. *Plant Cell* 14:421–433.
- Gray WM, Kepinski S, Rouse D, Leyser O, Estelle M (2001) Auxin regulates SCFTIR1-dependent degradation of AUX/IAA proteins. *Nature* 414:271–276.
- Read MA, *et al.* (2000) Nedd8 modification of cul-1 activates SCF(beta-TrCP)-dependent ubiquitination of IkkappaBalpha. *Mol Cell Biol* 20:2326–2333.
- Sakata E, *et al.* (2007) Direct interactions between NEDD8 and ubiquitin E2 conjugating enzymes upregulate cullin-based E3 ligase activity. *Nat Struct Mol Biol* 14:167–168.
- Gray WM, Hellmann H, Dharmasiri S, Estelle M (2002) Role of the Arabidopsis RING-H2 protein RBX1 in RUB modification and SCF function. *Plant Cell* 14:2137–2144.
- Cope GA, Deshaies RJ (2003) COP9 signalosome: A multifunctional regulator of SCF and other cullin-based ubiquitin ligases. *Cell* 114:663–671.
- Liu J, Furukawa M, Matsumoto T, Xiong Y (2002) NEDD8 modification of CUL1 dissociates p120(CAND1), an inhibitor of CUL1-SKP1 binding and SCF ligases. *Mol Cell* 10:1511–1518.
- Zheng J, *et al.* (2002) CAND1 binds to unneddylated CUL1 and regulates the formation of SCF ubiquitin E3 ligase complex. *Mol Cell* 10:1519–1526.
- Bornstein G, Ganoh D, Hershko A (2006) Regulation of neddylation and deneddylation of cullin1 in SCFSkp2 ubiquitin ligase by F-box protein and substrate. *Proc Natl Acad Sci USA* 103:11515–11520.
- Goldenberg SJ, *et al.* (2004) Structure of the Cand1-Cul1-Roc1 complex reveals regulatory mechanisms for the assembly of the multisubunit cullin-dependent ubiquitin ligases. *Cell* 119:517–528.
- Chuang HW, Zhang W, Gray WM (2004) Arabidopsis ETA2, an apparent ortholog of the human cullin-interacting protein CAND1, is required for auxin responses mediated by the SCF(TIR1) ubiquitin ligase. *Plant Cell* 16:1883–1897.
- Feng S, *et al.* (2004) Arabidopsis CAND1, an unmodified CUL1-interacting protein, is involved in multiple developmental pathways controlled by ubiquitin/proteasome-mediated protein degradation. *Plant Cell* 16:1870–1882.
- Hellmann H, *et al.* (2003) Arabidopsis AXR6 encodes CUL1 implicating SCF E3 ligases in auxin regulation of embryogenesis. *EMBO J* 22:3314–3325.
- Quint M, Ito H, Zhang W, Gray WM (2005) Characterization of a novel temperature-sensitive allele of the CUL1/AXR6 subunit of SCF ubiquitin-ligases. *Plant J* 43:371–383.
- Chen H, *et al.* (2006) Arabidopsis CULLIN4 forms an E3 ubiquitin ligase with RBX1 and the CDD complex in mediating light control of development. *Plant Cell* 18:1991–2004.
- Lo SC, Hannink M (2006) CAND1-mediated substrate adaptor recycling is required for efficient repression of Nrf2 by Keap1. *Mol Cell Biol* 26:1235–1244.
- Staub JM, Wei N, Deng XW (1996) Evidence for FUS6 as a component of the nuclear-localized COP9 complex in Arabidopsis. *Plant Cell* 8:2047–2056.
- Schwechheimer C, Deng XW (2000) The COP/DET/FUS proteins-regulators of eukaryotic growth and development. *Semin Cell Dev Biol* 11:495–503.
- Cope GA, *et al.* (2002) Role of predicted metalloprotease motif of Jab1/Csn5 in cleavage of Nedd8 from Cul1. *Science* 298:608–611.
- Cope GA, Deshaies RJ (2006) Targeted silencing of Jab1/Csn5 in human cells down-regulates SCF activity through reduction of F-box protein levels. *BMC Biochem* 7:1.
- Lincoln C, Britton JH, Estelle M (1990) Growth and development of the *axr1* mutants of Arabidopsis. *Plant Cell* 2:1071–1080.
- Witte CP, Noël LD, Gielbert J, Parker JE, Romeis T (2004) Rapid one-step protein purification from plant material using the eight-amino acid StrepII epitope. *Plant Mol Biol* 55:135–147.
- Ausubel FM (1994) *Current Protocols in Molecular Biology* (Wiley, New York).